RSC Advances

PAPER

View Article Online
View Journal | View Issue

Cite this: *RSC Adv.*, 2022, **12**, 12978

Parameter configuration of the electrical spark discharge method for preparing graphene copper nanocomposite colloids and the analysis of product characteristics

Kuo-Hsiung Tseng, *[a] Chang-Hsiang Huang,[a] Hsueh-Chien Ku,[a] Der-Chi Tien[a] and Leszek Stobinski[b]

The electrical spark discharge method was used to prepare graphene copper nanocomposite (GNS-Cu) colloids under normal temperature and pressure. Cu and graphite were mixed in deionized water at a Cu : C mass ratio of 9 : 1 (99% purity), and the mixture was used to produce composite rods as the electrodes for spark machining. An electrical discharge machine with five settings of pulse cycle turn-on and turn-off times, namely 10–10, 30–30, 50–50, 70–70, and 90–90 μs, was used to prepare five different types of GNS-Cu colloids. The ultraviolet-visible spectroscopy results revealed that the highest absorbance (2.441) was observed when the turn-on and turn-off times were 30–30 μs, indicating that this configuration was most efficient for preparing GNS-Cu colloids. Transmission electron microscopy and X-ray diffraction analysis were also conducted to examine the surface characteristics and crystal structure of GNS-Cu colloids. The transmission electron microscopy results revealed that Cu particles in the GNS-Cu colloids were located within or on top of graphene sheets. The Cu particle size varied with the discharge efficiency, and the lattice spacing of the Cu particles was approximately 0.218 nm. The results of X-ray diffraction analysis revealed that no byproducts were formed from the preparation of GNS-Cu colloids, which had complete crystal structures.

Received 5th March 2022
Accepted 20th April 2022

DOI: 10.1039/d2ra01456d

rsc.li/rsc-advances

1. Introduction

Graphene is a flat film comprising hexagonal lattices with carbon atoms with sp^2 orbitals. Because of its high thermal conductivity,[1] low resistivity, and favorable mechanical properties,[2,3] graphene is frequently applied in solar cells,[4] supercapacitors,[5] or reinforcing materials for composites.[6–8] Cu is a common metal with high thermal conductivity,[9] electrical conductivity,[10] and ductility. It is widely used to prepare nanoparticles for creating antibacterial agents.[11,12] Graphene and Cu have similar properties, enabling the use of these materials in combination to form composites. These composites can be used as oil-based additives for friction reduction[13] or mixed with epoxy resins to increase thermal conductivity.[14] Therefore, graphene and Cu are potential materials for practical applications as thermal interface materials and adhesives.

Graphene–Cu nanocomposite (GNS-Cu) can be prepared with chemical and physical methods; both are used in specific fields. Chemical methods, coating graphene films on copper nanoparticles by chemical vapor deposition, improved its mechanical properties and friction properties.[15] Electrochemical deposition of copper nanoparticles on graphene nanosheets, electrodes on sensors for detecting glucose and hydrogen peroxide, make the sensor have with good sensitivity and stability.[16] The graphene and copper nanoparticle composites prepared by *in situ* chemical reduction are used as electrodes for the detection of carbohydrate sensors, resulting in better sensitivity of the sensors,[17] are more common but also more costly than physical methods. However, the use of chemical agents can cause environmental pollution and harm human health. Therefore, effectively reducing the pollution and preparation costs associate with GNS-Cu synthesis is an essential topic. In this study, the electrical spark discharge method (ESDM)[18] was used to prepare GNS-Cu. The ESDM is an environmentally friendly physical method that is highly efficient with low costs and short preparation time. In this method, a servo control system is used to maintain two electrodes at an extremely short distance apart from one another,[19] and the duty cycle of voltage pulses is changed rapidly to generate a spark discharge that converts electrical energy to thermal energy. When sufficient thermal energy is generated, the electrode material melts and rapidly cools to form nanoparticles. ESDM is widely applied in precision processing to increase the precision

[a]*Department of Electrical Engineering, National Taipei University of Technology, Taipei 10608, Taiwan. E-mail: f10473@mail.ntut.edu.tw*

[b]*Faculty of Chemical and Process Engineering, Warsaw University of Technology, Waryńskiego 1, 00-645, Warsaw, Poland*

of the produced objects. The method can also be used to create nanosized colloids.[20–22] Five turn-on and turn-off time (T_{on}–T_{off}) settings were used to prepare GNS-Cu colloids. The quality of the resulting products was preliminary determined using ultraviolet-visible spectroscopy (UV-Vis). Next, the surface characteristics of the highest-quality products were examined using X-ray diffraction analysis (XRD) and transmission electron microscopy (TEM) to identify the optimal parameter configuration.

2. Experimental principles and methods

2.1 Experimental principles

An electrical discharge machine (EDM) was used to conduct the ESDM and prepare GNS-Cu. Fig. 1 presents the components of an EDM system, and Fig. 2 depicts the ESDM process for preparing nanosized colloids. Prior to discharge (Fig. 2(a)), the two electrodes were submerged in a dielectric fluid and maintained at a specific distance apart from each other. During this stage, the system is insulated, no voltage is applied, and neither gap voltage (V_{gap}) nor current (I_{gap}) are generated. On initiating the discharge process, the T_{on} period begins (Fig. 2(b)). In this period, the servo control system is used to adjust the distance between the two electrodes by maintaining them at an extremely short distance apart from one another. When the electric field strength on the electrode surface surpasses the insulation capacity of the dielectric fluid, a large number of electrons travel from the anode to cathode to form an electrical arc that generates a high temperature, inducing ionization (Fig. 2(c)). During this stage, electrons from the anode impact neutral atoms in the dielectric fluid and ionize them, forming cations. The electrons rapidly travel to the cathode, inducing the ionization effect to reduce V_{gap} and increase I_{gap}. Next, melting occurs (Fig. 2(d)). Under continuous ionization, the positive and negative ions continue to impact the two electrodes and form a high-temperature electrical arc between the electrodes. This process converts electrical energy to thermal energy, and the instantly-generated high temperature melts the Cu metal on the electrode surface. Cu nanoparticles detached from the electrode surface are dispersed and suspended in the dielectric fluid. The end of the discharge process is the T_{off} period (Fig. 2(e)) during which voltage is no longer applied to the two electrodes, V_{gap} and I_{gap} become zero, and the dielectric fluid returns to the insulating state. GNS-Cu particles are cooled in the dielectric fluid, and a spark machining cycle is completed. The dielectric fluid must completely return to the insulating state (Fig. 3(f)) before the next discharge processing cycle can begin. This process can be used to create nanoparticles.

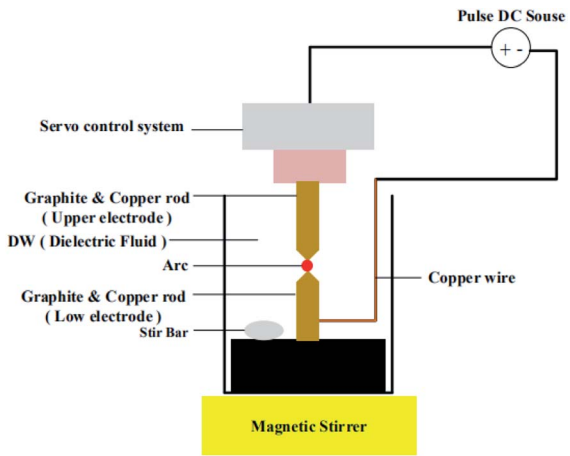

Fig. 1 Illustration of the spark machining process.

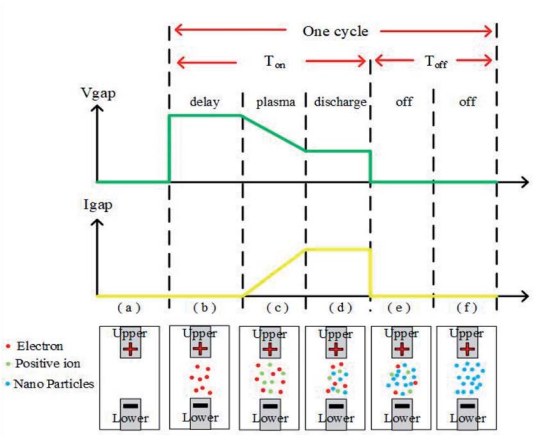

Fig. 2 Different stages of a spark machining process: (a) before discharge, (b) discharge initiation, (c) ionization, (d) electrode melting, (e) discharge termination, and (f) insulation recovery.

2.2 Experimental materials

Composite rods made of graphite and Cu were used as the upper and lower electrodes. The purity of the graphite and Cu used was 99%, and the Cu–C mass ratio of the composite rods was 9 : 1. Because electricity is discharged from electrode tips, the electrode diameter should be 1–2 mm. Graphite has a fragile

Fig. 3 Graphite–Cu composite rods.

structure and low ductility; consequently, graphite–Cu composite rods 1 to 2 mm in diameter are difficult to create; they also break easily. To address this problem, graphite rods with a diameter of 1 cm were first created. The rods were then sharpened on one end by using a grinder to achieve the small surface area required for discharge (Fig. 3). Because of its excellent insulation properties, deionized water was used as the dielectric fluid. The electrical conductivity of the water was 2.0 μs cm^{-1}.

2.3 Experimental methods

An EDM was used to prepare GNS-Cu, and different T_{on}–T_{off} settings were adopted to identify the optimal parameter configuration. Specifically, five T_{on}–T_{off} settings were used, namely 10–10, 30–30, 50–50, 70–70, and 90–90 μs. Table 1 presents the configuration of the other environmental parameters. The current segment was set to Level 3, and the high/low voltage switch was not activated. The no-load voltage was 140 V. The volume of dielectric fluid was 250 mL. The discharge time was 2 min. The preparation process was conducted at normal temperature and pressure. By using the above parameters, the graphite copper rods of the upper and lower electrodes are peeled off through the high-temperature spark discharge. This will form a graphene-copper composite colloid.

To compare the quality of GNS-Cu colloids created with different T_{on}–T_{off} settings, a preliminary optics analysis at the ultraviolet radiation range was conducted using a UV-Vis analyzer (9423UVA1002E Helios Omega). The optimal parameter configuration was then determined based on the analysis results. In general, absorbance values measured from UV-Vis are used to derive sample concentrations; a high absorbance value indicates a high concentration and therefore a successful discharge process. Because absorbance is unitless, only the absorbance values obtained from the same UV-Vis analyzer can be used to calculate concentrations. In this study, the GNS-Cu colloids prepared with the five T_{on}–T_{off} settings were analyzed to determine the optimal parameter configuration, and XRD (Empyrean) and TEM (HRTEM, JEM2100F) were performed for subsequent analysis. XRD was used to analyze the crystal structure, phase, and diffraction peaks of GNS-Cu, and the analysis results were used to determine the colloid composition. TEM was performed to determine the particle size, distribution, and lattice spacing. The XRD d-spacing data in the International Centre for Diffraction Data database were referenced to determine the particle phase.

Table 1 Configuration of environmental parameters

	Graphite, 99.9%
Material	Copper, 99.9%
Pulse cycle (T_{on}–T_{off})	10–10, 30–30, 50–50, 70–70, 90–90 (μs)
Current segment (IP)	3
Voltage (V)	140
Fluid (mL)	DW, 250
Discharge time (min)	2
Temperature (°C)	25

3. Results and discussion

3.1 UV-Vis results

This study adopted five T_{on}–T_{off} settings (10–10, 30–30, 50–50, 70–70, and 90–90 μs) to prepare the GNS-Cu with a discharge time of 2 min. Fig. 4 presents the UV-Vis spectra of the colloids. The results revealed that the characteristic peaks of the colloids all appeared at 219 nm. Thus, changing the T_{on}–T_{off} setting did not affect the optical properties of the product. Table 2 lists the absorbance values of the colloids prepared for 10–10, 30–30, 50–50, 70–70, and 90–90 μs, which were 2.171, 2.441, 2.329, 2.231, and 1.873, respectively. In particular, the colloid prepared for 30–30 μs had the highest absorbance, indicating that this discharge process was the most successful. Therefore, this setting is the most suitable for GNS-Cu preparation.

3.2 XRD pattern results

Fig. 5 presents the XRD results, which revealed that the prepared GNS-Cu had three crystal phases, namely C (00-041-148), Cu (00-001-083), and CuO (01-089-2529). The Bragg angle and crystal plane of graphite are 26° and (002), respectively. The Bragg angles of Cu are 43°, 50°, and 74°, and its crystal planes are (111), (200), and (220). The Bragg angles of CuO are 35° and 38°, and its crystal planes are (−111) and (111). Because only these characteristics were observed in the XRD spectrum, the prepared GNS-Cu was verified to contain only the crystal structures of C, Cu, and CuO, and no other byproducts were formed.

3.3 TEM image results

TEM was conducted to observe the particle size, shape, and distribution using a nickel mesh with a discontinuous carbon

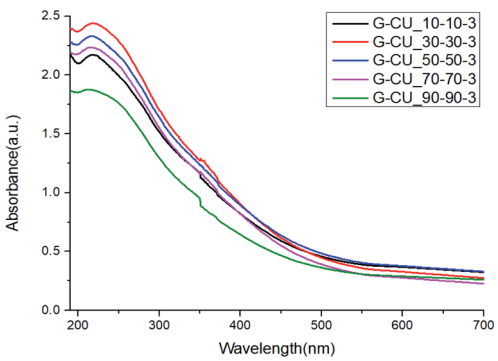

Fig. 4 UV-Vis spectra of the colloids prepared with different T_{on}–T_{off} settings.

Table 2 Absorbance values of the colloids prepared with different T_{on}–T_{off} settings

T_{on}–T_{off} (μs)	Absorbance
10–10 μs	2.171
30–30 μs	2.441
50–50 μs	2.329
70–70 μs	2.231
90–90 μs	1.873

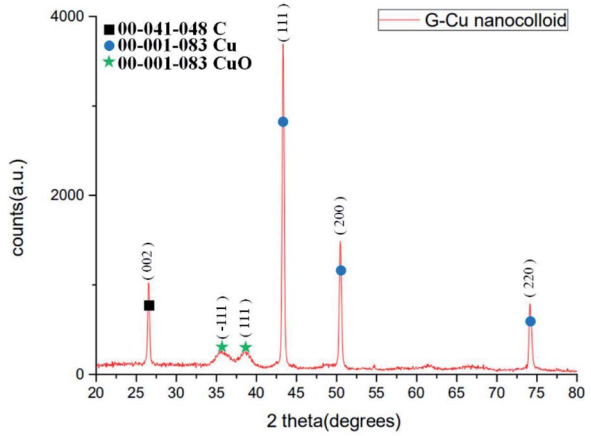

Fig. 5 XRD spectrum of the prepared GNS-Cu.

film as a carrier. The results revealed that the colloid samples contained both C and Cu, which did not form compounds. Fig. 6(a) presents the TEM image with a scale bar of 100 nm. Irregularly-shaped translucent graphene sheets can be observed in this image. The black particles of varying size are Cu nanoparticles. The diameter of the particles in the left region of the image is larger because the discharge efficiency was poorer. Fig. 6(b) presents a magnified image (scale bar of 50 nm) of the white square region in Fig. 6(a). The image verifies that the Cu nanoparticle is located on top of the graphene sheet; the particle size was determined to be approximately 50 nm. Fig. 6(c) presents the magnified image (scale bar of 10 nm) of the white square region in Fig. 6(b). The black area in the image is the copper nanoparticles; the lattice lines can be clearly observed. The lattice spacing was measured as 0.218 nm.

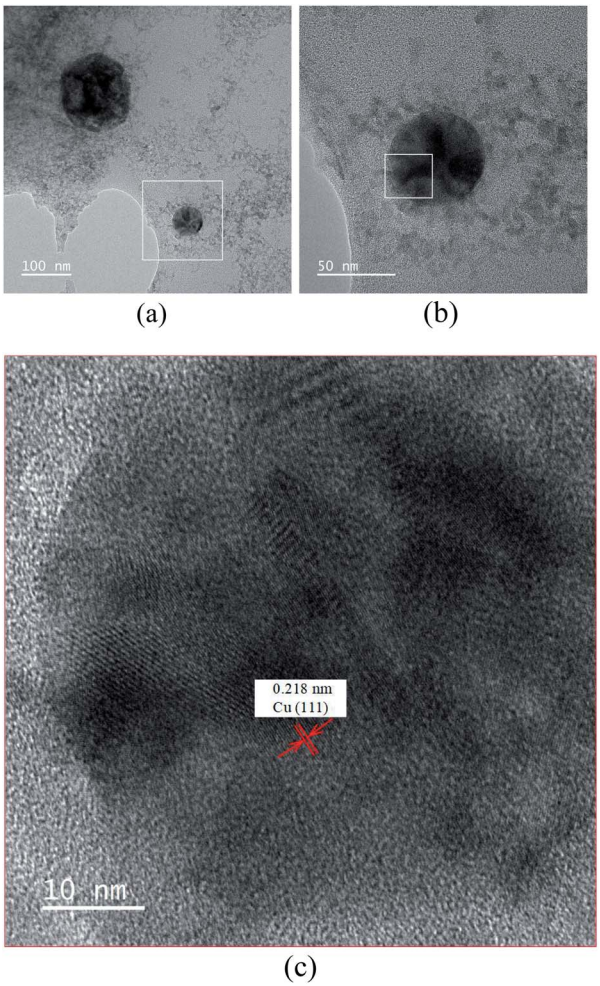

Fig. 6 TEM images of -GNS-Cu. Scale bars are (a) 100 nm, (b) 50 nm, and (c) 10 nm.

Different T_{on}–T_{off} settings were adopted to prepare GNS-Cu through the ESDM and identify the optimal parameter configuration. The UV-Vis results verified that 30–30 μs yielded the highest absorbance (2.441) and discharge efficiency. The XRD results revealed that the prepared GNS-Cu colloid only had C, Cu, and CuO crystal structures, and no byproducts were created. TEM revealed that Cu particles were located on top of the translucent graphene sheets. The Cu particle size varied with the discharge efficiency. The actual measurement of the Cu lattice spacing was 0.218 nm.

4. Conclusions

This study was the first to adopt ESDM and an EDM to prepare GNS-Cu colloids at standard pressure and temperature without using any dispersants or additional chemical reagents. The optimal T_{on}–T_{off} setting was identified using UV-Vis. The results verified that ESDM is a low-cost, efficient, and green process for GNS-Cu preparation. This study contributes to the relevant body of knowledge in the following areas:

(1) ESDM can be used to prepare GNS-Cu at standard temperature and pressure, and no dispersants or additional chemical reagents are required. Compared with other methods, ESDM causes less pollution and fewer negative effects on human health. It is a rapid and green preparation process.

(2) UV-Vis verified that when T_{on}–T_{off} was set to 30–30 μs, the characteristic peak of the GNS-CU prepared with the ESDM appeared at 219 nm and the absorbance was 2.441.

(3) The XRD results confirmed the presence of graphene, Cu, and CuO crystal phases and Bragg angles in the prepared colloid, verifying that the product indeed contained graphene and Cu. However, the formulation of oxides during the process was inevitable.

(4) TEM was conducted to observe the GNS-Cu microscopically and to measure the lattice spacing, which was then compared with that determined using the XRD. The results revealed that the prepared colloids contained both graphene and Cu nanoparticles. Irregular lattice lines were also observed; these were caused by the interference between Cu and graphite.

Funding

The Ministry of Science and Technology (MOST 109-2221-E-027-063-).

Author contributions

Project administration, Kuo-Hsiung Tseng; resources, Kuo-Hsiung Tseng; supervision, Kuo-Hsiung Tseng; funding acquisition, Kuo-Hsiung Tseng; data curation, Chang-Hsiang Huang and Hsueh-Chien Ku; formal analysis, Chang-Hsiang Huang; methodology, Der-Chi Tien; validation, Der-Chi Tien, and Leszek Stobinski; writing–original draft, Chang-Hsiang Huang and Hsueh-Chien Ku; writing–review & editing, Der-Chi Tien, and Leszek Stobinski. All authors have read and agreed to the published version of the manuscript.

Conflicts of interest

The authors declare no conflict of interest.

Acknowledgements

The authors would like to thank the Precision Research and Analysis Center, National Taipei University of Technology for technical supporting this research.

References

1 C. Lee, X. Wei, J. W. Kysar and J. Hone, Measurement of the elastic properties and intrinsic strength of monolayer graphene, *Science*, 2008, **321**(5887), 385–388.
2 A. A. Green and M. C. Hersam, Emerging methods for producing monodisperse graphene dispersions, *J. Phys. Chem. Lett.*, 2010, **1**(2), 544–549.
3 A. K. Geim, Graphene: status and prospects, *Science*, 2009, **324**(5934), 1530–1534.
4 Z. Y. Li, M. S. Akhtar, J. H. Kuk, B. S. Kong and O. B. Yang, Graphene application as a counter electrode material for dye-sensitized solar cell, *Mater. Lett.*, 2012, **86**, 96–99.
5 G. Abellán, E. Coronado, C. Martí-Gastaldo, A. Ribera and T. F. Otero, Magnetic nanocomposites formed by FeNi3 nanoparticles embedded in graphene. Application as supercapacitors, *Part. Part. Syst. Charact.*, 2013, **30**(10), 853–863.
6 S. F. Bartolucci, J. Paras, M. A. Rafiee, J. Rafiee, S. Lee, D. Kapoor and N. Koratkar, Graphene–aluminum nanocomposites, *Mater. Sci. Eng. A*, 2011, **528**(27), 7933–7937.
7 S. Hai-Yang and Z. Xin-Wei, Mechanical properties of Ni-coated single graphene sheet and their embedded aluminum matrix composites, *Commun. Theor. Phys.*, 2010, **54**(1), 143.
8 T. S. Koltsova, L. I. Nasibulina, I. V. Anoshkin, V. V. Mishin, E. I. Kauppinen, O. V. Tolochko and A. G. Nasibulin, New hybrid copper composite materials based on carbon nanostructures, *J. Mater. Sci. Eng. B*, 2012, **2**(4), 240–246.
9 X. Wei, H. Zhu, T. Kong and L. Wang, Synthesis and thermal conductivity of Cu2O nanofluids, *Int. J. Heat Mass Transfer*, 2009, **52**(19–20), 4371–4374.
10 K. Han, R. P. Walsh, A. Ishmaku, V. Toplosky, L. Brandao and J. D. Embury, High strength and high electrical conductivity bulk Cu, *Philos. Mag.*, 2004, **84**(34), 3705–3716.
11 U. Bogdanović, V. Lazić, V. Vodnik, M. Budimir, Z. Marković and S. Dimitrijević, Copper nanoparticles with high antimicrobial activity, *Mater. Lett.*, 2014, **128**, 75–78.
12 S. Wu, S. Rajeshkumar, M. Madasamy and V. Mahendran, Green synthesis of copper nanoparticles using Cissus vitiginea and its antioxidant and antibacterial activity against urinary tract infection pathogens, *Artif. Cells, Nanomed., Biotechnol.*, 2020, **48**(1), 1153–1158.
13 X. Li, Y. Zhao, W. Wu, J. Chen, G. Chu and H. Zou, Synthesis and characterizations of graphene–copper nanocomposites and their antifriction application, *J. Ind. Eng. Chem.*, 2014, **20**(4), 2043–2049.
14 Z. Barani, A. Mohammadzadeh, A. Geremew, C. Y. Huang, D. Coleman, L. Mangolini and A. A. Balandin, Thermal properties of the binary-filler hybrid composites with graphene and copper nanoparticles, *Adv. Funct. Mater.*, 2020, **30**(8), 1904008.
15 S. Wang, S. Han, G. Xin, J. Lin, R. Wei, J. Lian and Q. Yu, High-quality graphene directly grown on Cu nanoparticles for Cu–graphene nanocomposites, *Mater. Des.*, 2018, **139**, 181–187.
16 V. Mani, R. Devasenathipathy, S. M. Chen, S. F. Wang, P. Devi and Y. Tai, Electrodeposition of copper nanoparticles using pectin scaffold at graphene nanosheets for electrochemical sensing of glucose and hydrogen peroxide, *Electrochim. Acta*, 2015, **176**, 804–810.
17 Q. Chen, L. Zhang and G. Chen, Facile preparation of graphene–copper nanoparticle composite by in situ chemical reduction for electrochemical sensing of carbohydrates, *Anal. Chem.*, 2012, **84**(1), 171–178.
18 K. H. Ho and S. T. Newman, State of the art electrical discharge machining (EDM), *Int. J. Mach. Tool Manufact.*, 2003, **43**(13), 1287–1300.
19 K. H. Tseng, Y. S. Lin, Y. C. Lin, D. C. Tien and L. Stobinski, Deriving optimized PID parameters of nano-Ag colloid prepared by electrical spark discharge method, *Nanomaterials*, 2020, **10**(6), 1091.
20 K. H. Tseng, H. C. Ku, D. C. Tien and L. Stobinski, Parameter control and concentration analysis of graphene colloids prepared by electric spark discharge method, *Nanotechnol. Rev.*, 2019, **8**(1), 201–209.
21 K. H. Tseng, H. C. Ku, D. C. Tien and L. Stobinski, Novel preparation of reduced graphene oxide–silver complex using an electrical spark discharge method, *Nanomaterials*, 2019, **9**(7), 979.
22 K. H. Tseng, Z. Y. Lin, M. Y. Chung, D. C. Tien and L. Stobinski, Parameter control and property analysis in the preparation of platinum iodide nanocolloids through the electrical spark discharge method, *RSC Adv.*, 2020, **10**(50), 30169–30175.